

# Properties of Cement Pastes Doped with Very High Amounts of Ground Granulated Blast-Furnace Slag

A. M. Rashad

\* a.rashad@hbrc.edu.eg

Received: October 2017

Accepted: February 2018

<sup>1</sup> Building Materials Research and Quality Control Institute, Housing & Building National Research Center, HBRC, Cairo, Egypt.

DOI: 10.22068/ijmse.15.2.1

**Abstract:** In the current work, the properties of cement pastes doped with high amounts of ground granulated blast-furnace slag (HVS) were investigated. Portland cement (PC) was substituted with ground granulated blast-furnace slag (donated as slag) at very high amounts of 85%, 90%, 95% and 100%, by weight. PC paste without any content of slag was used as a reference. Some fresh and hardened properties such as workability, density, compressive strength up to 56 days, pH value and drying shrinkage up to 200 days were measured. The various phases formed were identified using X-ray diffraction (XRD) and thermogravimetric analysis (TGA). The microstructure of the formed hydration products was determined by scanning electron microscopy (SEM). The results indicated that HVS has higher workability and higher drying shrinkage beyond 60 days. On the other hand, HVS has lower pH, density and compressive strength.

**Keywords:** High volume slag, Workability, pH value, Density, Compressive strength, Drying shrinkage.

## 1. INTRODUCTION

Concrete is the most used construction material on the Earth. The annual production of concrete is almost 12 billion tonnes [1]. The production of vast amounts of PC occasionally results in environmental problems in term of energy consumption as well as pollution [2]. PC production represents approximately from 74% to 81% of the total CO<sub>2</sub> emissions of concrete. The production of 1 tonne of PC generates about 0.94 tonnes of CO<sub>2</sub>. This large amount of carbon dioxide is generated by four different sources. 40% of this emission caused by the fossil fuel, 10% is contributed due to raw material transportation as well as electricity generation and the remaining (almost 50% of total emission in cement plant) is generated by decomposition of limestone. The PC industry not only releases CO<sub>2</sub>, but also releases SO<sub>3</sub> and NO<sub>x</sub> which can cause the greenhouse effect and acid rain [3-7]. These cause about 20% variations for the global warming [8]. PC is produced by a highly energy intensive process [9, 10], where the thermal energy required for clinkering is about 3.06 GJ fuel energy per tonne of clinker (in dry process), whereas some older wet process plants can

consume more than twice that amount [11]. PC accounts the third largest use of energy, after that of aluminium and steel manufacturing industries [1]. In addition, PC industry consumes a lot of virgin materials where producing each tonne of PC in which about 1.5 tonnes of raw materials are needed [1, 3-5, 7].

Increasing the use of supplementary cementitious materials (SCM) such as slag, fly ash (FA) and silica fume (SF) in concrete is an obvious and necessary step to reduce carbon dioxide emission [12]. These waste materials possessed hydraulic or/and pozzolanic properties and when used at optimal levels, enhanced mechanical performance and durability. Incorporation these by-products in concrete reduced the environmental impact of concrete by reducing the PC consumption and reducing the content of inert filler. In the literature, there are numerous researches related to the use of slag in concrete, mortar or paste as cement replacement typically at levels between 20% to 50% [13,14] and rarely exceed 60% [15-18]. In fact, there are limitations in the use of the SCM as replacement exceeding 60%.

In this investigation, PC was replaced with slag at large levels of 85%, 90%, 95% and 100%.

Some properties of the studied mixtures were investigated such as workability, pH value, compressive strength, density and drying shrinkage. The various phases formed were identified using X-ray diffraction (XRD) and thermogravimetric analysis (TGA). The microstructure of the formed hydration products was determined by scanning electron microscopy (SEM). Moreover, this paper aims to respond extra four issues: lower emission of pollutants into atmosphere by replacing PC with large volume of slag, reduction in consumption of natural resources required in PC industry, reduction the amount of fuel required in PC industry and eliminate the slag disposal. Really, this investigation will therefore add valuable knowledge in the field of HVS.

## 2. EXPERIMENTAL

### 2. 1. Materials

Portland cement, CEMI Class 42.5R, with a Blaine surface area of 270 m<sup>2</sup>/kg (complies with EN 197-1: 2001), was used as a reference. Ground granulated blast-furnace slag (GGBS) "donated as slag" was supplied by UK Hanson Cement was used as the raw material to produce the HVS pastes. The Blaine surface area of the slag is 300 m<sup>2</sup>/kg. The chemical compositions of the PC and slag were determined by X-ray fluorescence (XRF) and the results are shown in Table 1, whilst Fig 1 shows the mineral compositions of the slag.

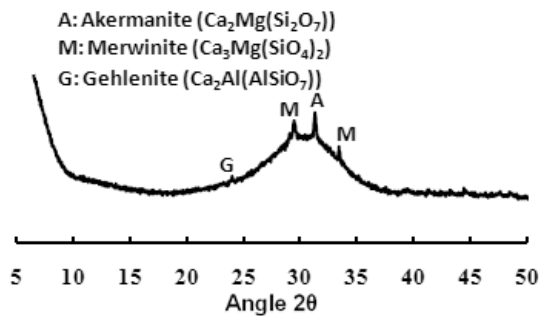


Fig.1. XRD pattern for the slag

Table 1. Oxide composition of PC and slag (% by mass) after calculation from XRF results

Composition	PC	slag
CaO	63.47	42.54
SiO <sub>2</sub>	20.18	35.69
Al <sub>2</sub> O <sub>3</sub>	4.83	11.81
MgO	2.47	7.63
Fe <sub>2</sub> O <sub>3</sub>	3.16	0.9
SO <sub>3</sub>	3.26	0.79
K <sub>2</sub> O	0.52	0.28
Na <sub>2</sub> O	0.16	0.16
TiO <sub>2</sub>	0.3	0.49
MnO	0.22	0.21
P <sub>2</sub> O <sub>5</sub>	0.09	0.01
CaCO <sub>3</sub>	-	-
Cl <sup>-</sup>	-	-
Loss of ignition	2.18	-1.09
Total	100.34	100.49

### 2. 2. Mixture Proportions

Five different mixtures were prepared. The first mixture was prepared from neat PC without any content of slag. The remaining four mixtures were prepared from composition of slag, with very high volume, with or without PC. The PC was replaced with slag at large levels of 85%, 90%, 95% and 100%, by weight. All mixing proportions are detailed in Table 2. A water binder ratio (w/b) of 0.3 was fixed for all mixtures.

Table 2. Details of mixture proportions

Mixture	PC (%)	Slag (%)
GS0	100	0
GS85	15	85
GS90	10	90
GS95	5	95
GS100	0	100

### 2. 3. Method

The cementitious materials were formulated with PC/slag ratios of 100/0, 15/85, 10/90, 5/95 and 0/100. Cementitious materials were mixed

for 4 min in mechanical mixture with a working speed of 80 rpm to ensure homogeneous mixing. The water was added and mixed with the cementitious materials for 5 min period followed by 2 min resting and any unmixed powders were scraped from the sides and paddle into the mixing bowl. Additional 5 min mixing was continued before casting. After mixing, the fresh pastes were immediately poured into  $50 \times 50 \times 50 \text{ mm}^3$  moulds and vibrated for 1 min to remove air voids. Immediately after casting, the moulds were covered with a wet hessian and sealed in a plastic sample bag. All specimens were then cured in an environmental chamber at  $40 \pm 1^\circ\text{C}$  for 3 days before removing the cubes from the steel moulds. Each cube was then again wrapped with a damp hessian cloth, sealed in a plastic sample bag and cured at  $40 \pm 1^\circ\text{C}$  until testing. The damp hessian cloth was regularly checked and replaced if became dry.

Paste workability was measured using a mini-slump test. In this test, a small cone with a bottom diameter of 38.1 mm, a top diameter of 19 mm and a height of 52.7 mm [9, 10] in the center of a square piece of smooth plastic, was used. The cone was filled with the paste and then lifted. The spread diameter is then measured in two perpendicular directions and the average spread was reported.

The compressive strength of samples hydrated for 3, 7, 28, and 56 days was measured in triplicate in accordance with ASTM C109/C109M-16a. A universal compressive strength testing machine with a constant load rate of 50 kN/min and 100 kN capacity was used to measure the compressive strength of the cubes. The density of the hardened paste at saturated surface dried condition was measured in accordance with BS 1881: Part 114: 1983 [19] at age of 28 days. After compressive strength testing, the debris from the crushed specimens have been stored in acetone in order to stop their hydration. After being stored in the acetone for three days, the debris were filtered from the acetone and then dried in a desiccator under vacuum. Part of the dried samples was ground in an agate mortar. Particles passing a  $63 \mu\text{m}$  sieve were used for X-ray diffraction (XRD) and thermogravimetric (TGA) analysis. Selected pieces were also used for the scanning electron microscopy (SEM) analysis.

The extra powder sample as obtained for the

XRD test was used to measure the pH of the hardened pastes at the age of 28 days. Solution samples were prepared with 1 part of powder and 10 parts of water. These powder/water mixes were kept rotating on a roller table for 24 h after which time they were placed in a centrifuge operating at 5000 rpm for 5 min to separate the solids from the liquid. The liquid was transferred to a new bottle where the pH was measured using a hand held pH probe.

The shrinkage prisms had 25 mm square cross-section and 285 mm length. Four to eight prism specimens were prepared for selected mixtures. The prisms were demoulded after 3 days from casting. The shrinkage prisms were stored afterwards in the drying room at  $20 \pm 1^\circ\text{C}$  and  $50 \pm 5\%$  RH. The first reading of the length was taken at the fourth day. Changes in the lengths were monitored every 7 days up to 200 days.

A PANalytical's XPert Pro X-ray diffractometer with nickel-filtered  $\text{CuK}\alpha 1$  radiation  $1.5405 \text{ \AA}$ , 40kV voltage and 40mA current with scanning speed of 0.50/min and step size of 0.020/min was used to identify crystalline phases presented in the samples. A Simultaneous Thermal Analyser STA 449 C Jupiter was employed to measure some material physical properties as a function of temperature change. For thermogravimetric analysis (TGA), the samples were heated in an atmosphere of nitrogen at  $10^\circ\text{C}/\text{min}$  up to  $1000^\circ\text{C}$ . Scanning electron microscope (SEM) fitted with EDAX unit was used to examine the microstructure of some reference and heated samples.

### 3. RESULTS AND DISCUSSION

#### 3. 1. Workability

The slump of HVS increased as the slag content increased (Fig. 2). The mixture of GS100 showed the highest workability, whilst the mixture of GS0 showed the lowest workability. Most of the previous investigations showed higher workability of slag blended cement in comparison with that of neat cement. Wei et al. [20] showed that as slag content in concrete increased the water required for standard pastes decreased. Rashad et al. [13] reported that concrete with either 10% or 20% slag as cement replacement exhibited higher workability than

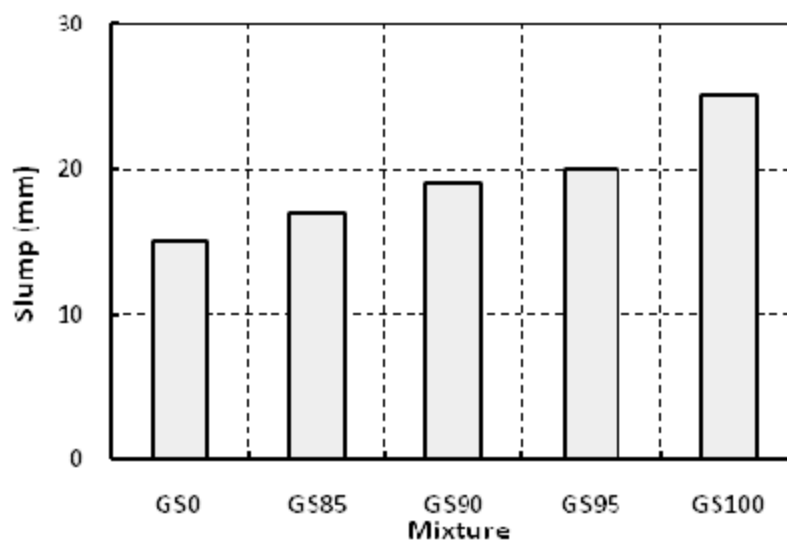


Fig. 2. Mini slump for various mixtures

that of control concrete. However, although, like cement, slag is a crushed material and therefore angular in shape, its surface is much smoother than that of cement, and this should result in an improvement in workability. In addition, because slag has a slightly lower relative density than PC (2.9 compared to 3.1), replacement on an equal weight to weight basis will result in an increase in powder volume which again should lead to an increase in workability. Linnu et al. [21] related the positive effect of HVS on the workability of mixture to the decrease of CaO which can be consumed and mitigated its negative impact on the workability by slag. The improving workability with the incorporation of slag could be relevant to the better dispersion and the slag particles surface properties, which are smooth and dense. Consequently, slag particles absorb little water.

### 3. 2. pH Value

Generally, the values of pH are important to keep the high alkalinity that leads to a passive layer formed on reinforced steel that reduce corrosion attack to negligible values. However, Fig. 3 shows the pH value of the neat PC sample and HVS samples at age of 28 days. It can be seen that the GS0

gave the highest pH value (12.74). When PC was replaced with 85% slag, pronounced reduction in pH value was observed. The pH value of GS85 reached about 12.36. As slag content increases as the pH value decreases. The lowest pH value was observed for GS100 which reached 12.23. This value is still higher enough to enable the passive layer forming on the steel bars.

### 3. 3. Compressive Strength

The compressive strength of the studied HVS

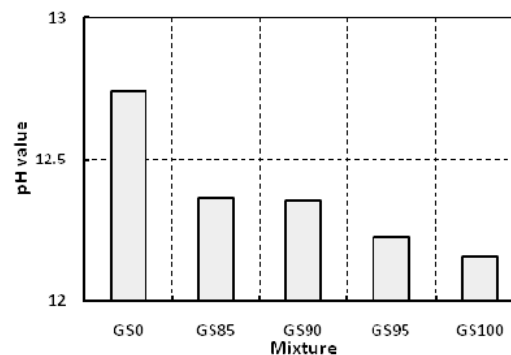


Fig. 3. pH value for pastes made with PC and HVS at age of 28 days

mixtures in addition to the neat PC mixture after 3, 7, 28 and 56 days of hydration are presented in Fig. 4. The values reported are the mean of three cubes. The compressive strength increased for all mixtures with increasing curing time. This is attributed to the increase of the amount of hydrated products. The pastes with HVS exhibited lower compressive strength than that of the neat PC paste at all ages, as expected. The strength values for the neat PC and HVS pastes ranged from 81.96 MPa (at age of 3 days) to 116.1 MPa (at age of 56 days), whilst these values ranged from 2.21-49.26 MPa (at age of 3 days) to 33.1-63.64 MPa (at age of 56 days), respectively, depending mainly on slag content.

At age of 3 days, the replacement of PC with 100% slag (GS100) exhibited the lowest compressive strength among all studied mixtures. When the PC was replaced with 95% slag, the compressive strength at age of 3 days increased about 7 times in comparison with that of GS100. As the content of slag decreased from 95% to 90%, further increase in the compressive strength was observed. The 3 days compressive strength of GS90 reached 16.48 and 2.35 times greater than that of GS100 and GS95, respectively. Further decrease in slag content up to 85%, led to further increase in the compressive strength gap related to GS100. The compressive strength of GS85, at age of 3 days, reached 23.24 times greater than that of GS100. Obviously from Fig.

4 it can be seen that as the curing time extended, the gap of compressive strength between GS100 and other HVS mixtures decreased. The compressive strength values of GS90 were 1.94 and 1.33 times greater than that of GS100, at age of 28 and 56 days, respectively. On the same line, the compressive strength values of GS85 were 2.67 and 1.92 times greater than that of GS100 at ages of 28 and 56 days, respectively. On the contrary, GS95 showed lower compressive strength than that of GS100 at ages of 28 and 56 days. Obviously from Fig. 4, the 3 days compressive strength of GS0 mixture is about 74.68% of its 28 days compressive strength, whilst it is about 9.53% for the paste mixture with 100% slag (GS100). The difference of the strength gain vanishes with time. At 7 days, pastes with 100% slag level developed about 36.78% of its 28 days strength, whilst it reached about 78.99% for 100 PC paste. It is well known that the hydration of slag blended cement occurs over an extended period of time as it relies on the release of calcium hydroxide from the hydration of PC. Therefore, at the early ages, the internal structure of slag paste tends to more porous than that of PC paste. Hence more gap of compressive strength between slag pastes and neat PC paste at early ages compared to latter ages was observed. In addition, the initial rate of reaction between slag and water is slower than that of PC and water, which means that the strength development is also be slower.

Percentage of strength reductions of the HVS pastes compared with the neat PC paste is summarized in Table 3. With 85% slag, the compressive strength decreased by 39.9%, 41.15%, 45.82% and 45.19% at 3, 7, 28 and 56 days, respectively. In previous investigation, Atiş and Bilim [22] found 44.22% reduction in the 28 days compressive strength in concrete containing 80% slag at cement replacement at w/b ratio of 0.5, when the curing condition was wet curing. Güneysi and Gesoğlu [23] found 40.91% reduction in the 28 days compressive strength in concrete containing 80% slag (with Blaine surface area 404 m<sup>2</sup>/kg) as cement replacement at w/b ratio of 0.4, when the curing condition was air curing. Miura and Iwaki [24] found 55.76% reduction in the 28 days compressive strength in

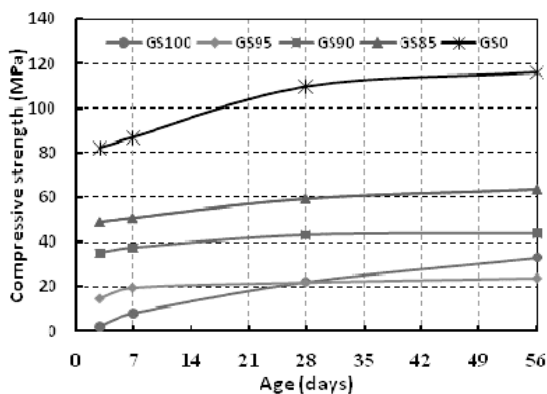


Fig. 4. Compressive strength development of PC and HVS pastes

**Table 3.** Percentage of strength reduction with GS0

Mixture	3 days	7 days	28 days	56 days
GS85	39.897	41.149	45.818	45.185
GS90	57.36131	56.92095	60.7119	62.22796
GS95	81.89361	77.37619	80.04616	79.50043
GS100	99.97413	99.90564	99.79736	99.71519

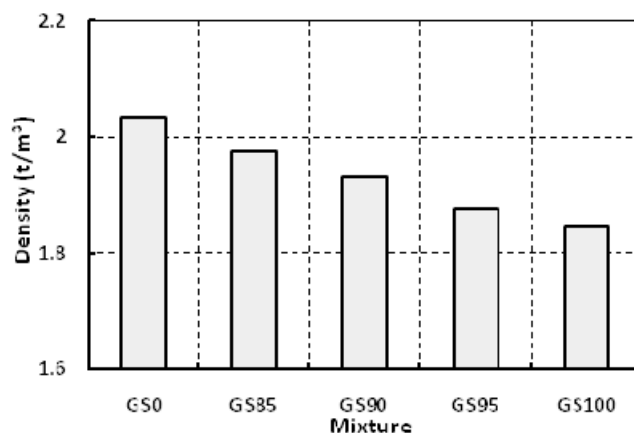
mortar containing 80% slag as cement replacement at w/b ratio of 0.5, when the curing condition was air curing at 20 °C.

The reductions in the compressive strength due to the incorporation of 90% slag was 57.36%, 56.92%, 60.71% and 62.23% at 3, 7, 28 and 56 days, respectively. This reduction increased with increasing slag content in which it reached 99.97%, 99.91%, 99.8% and 99.72% at ages of 3, 7, 28 and 56 days, respectively, for pastes had 100% slag (GS100). The results of strength values at latter ages indicated that there was continuous improvement in strength beyond age of 7 days. The increase in compressive strength from 7 days to 28 days was 16.56%, whereas the increase in compressive strength from 7 days to 56 days was 24.74%, for GS85. For GS90, this improvement was 15.55% and 17.42% from 7 days to 28 days and from 7 days to 56 days, respectively. The GS100 showed the best improvements in comparison with other studied mixtures where the increase in compressive strength

from 7 days to 28 days reached 171.88% and the increase in compressive strength from 7 days to 56 days reached 304.24%. Apparently, from Fig. 4 it can be seen that the compressive strength of GS95 is higher than that of GS100 at ages of 3 and 7 days. The enhancement in the compressive strength of GS95 over that of GS100 was 600% and 139.77% at ages of 3 and 7 days, respectively. On the contrary, after 28 days of hydration, the compressive strength of GS100 seemed to be comparable to that of GS95. The compressive strength of GS100 at age of 56 days was approximately 1.40 times greater than that of GS95, this notation still needs more investigations.

### 3. 4. Density

The density of hardened paste at saturated surface dried condition was measured at age of 28 days. From the results in Fig. 5, it can be seen that the density of the hardened pastes decreased

**Fig. 5.** Paste density at saturated surface dry condition at age of 28 days

with increasing slag content. The highest value of specific gravity was found for GS0, whilst the GS100 showed the lowest value. The specific gravity of GS0 was about 1.1 time greater than that of GS100. This is due to the lower specific gravity of the slag in comparison with that of the cement.

### 3. 5. Crystalline Phases

XRD technique was used to acquire a better understanding of the possible transformations underway in the original material as well as the samples containing HVS. Figs. 6, 7 present the XRD traces of neat PC and HVS paste samples

after 28 days of hydration. Fig. 6 show the XRD pattern of the neat PC sample (GS0) which indicating the hydration products. The expected crystalline hydration products are clearly evident. Portlandite  $\text{Ca(OH)}_2$  was formed in appreciable amounts as a good crystalline reaction product. The semi crystalline CSH gel which overlapped with calcite was also formed (main peak at  $29.4^\circ 2\theta$ ). The amount of unhydrated  $\text{C}_3\text{S}$  and  $\beta\text{-C}_2\text{S}$  were detected. Appreciable amounts of ettringite ( $\text{Ca}_6\text{Al}_2(\text{SO}_4)_3(\text{OH})_{12} \cdot 26\text{H}_2\text{O}$ ) were detected. No other phases were identified in the XRD patterns.

Fig. 7 shows that the HVS paste samples with or without different contents of PC had a diffuse

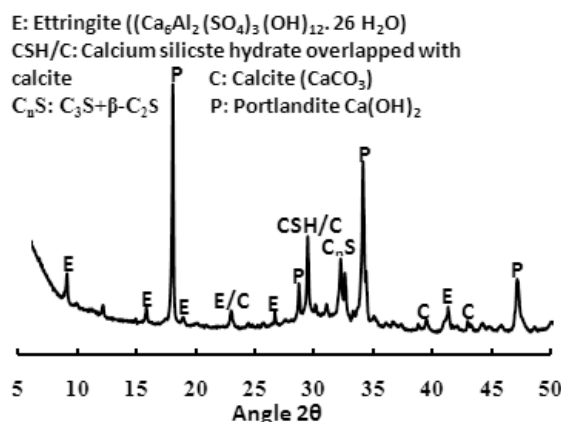


Fig. 6. X-ray patterns of neat PC paste after 28 days of hydration

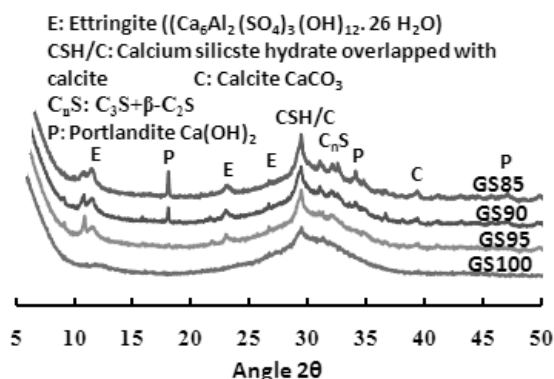


Fig. 7. X-ray patterns of HVS pastes after 28 days of hydration

hump at about  $30^\circ 2\theta$ . In HVS without any PC content (GS100), the XRD of this sample does not contain either portlandite (CH) or ettringite ( $\text{Ca}_6\text{Al}_2(\text{SO}_4)_3(\text{OH})_{12}\cdot 26\text{H}_2\text{O}$ ). The semi crystalline CSH gel, which overlaps with calcite, could be seen in all slag samples and the intensity of this peak increased slightly with the increase in PC content. The highest intensity of the CSH peak which overlaps with calcite was found in GS85 sample followed by GS90 sample. This may be a part of the reason why GS85 exhibited higher compressive strength in comparison with those of GS90. However, in HVS paste samples containing either 10% or 15% PC (GS90 and GS85), ettringite, portlandite and CnS ( $\text{C}_3\text{S} + \beta\text{-C}_2\text{S}$ ) were detected. The intensity of portlandite slightly increased with increasing PC content. In addition, the intensity of ettringite also increased with increasing PC content. In HVS paste sample containing 5% PC (GS95), ettringite and very little amount of CnS were detected.

### 3. 6. Thermogravimetric Analysis

Thermogravimetric analysis (TGA) and derivative thermogravimetry (DTA) were used to assess the rates of water evaporation in a system or identify the mechanism by which a material loses weight as a result of controlled heating [25, 26]. The samples were submitted to a controlled heating process in  $\text{N}_2$  atmosphere between 25 and

1000  $^\circ\text{C}$ . The TGA/DTG of the neat PC sample (GS0) after 28 days of hydration is presented in Fig. 8. As shown, three main endothermic peaks can be identified. The first peak located at approximately 110-120  $^\circ\text{C}$ , is mostly due to the decomposition of CSH and ettringite [9]. The second peak at the region of 400-500  $^\circ\text{C}$ , which indicated the decomposition of portlandite (CH) [27, 28]. The third peak at approximately 740  $^\circ\text{C}$  is due to the decarboxylation of calcite [9].

Fig. 9 presents the TGA/DTG of hardened HVS pastes after 28 days of hydration. As can be seen from the DTG diagram, when the samples of GS85, GS90, GS95 and GS100 were heated up to 1000  $^\circ\text{C}$ , the endothermic peak appeared at approximately 90-120  $^\circ\text{C}$  is due to the decomposition of CSH and ettringite (for GS85, GS90 and GS95). For GS100 sample, the endothermic peak which appeared at 90-120  $^\circ\text{C}$  is due to the decomposition of CSH. The peak that appeared at approximately 500  $^\circ\text{C}$  in GS85 and GS90 samples, is due to the decomposition of  $\text{Ca}(\text{OH})_2$ . For GS90 and GS85 samples, there are too minor peaks. One of them which appeared at between ~400-500  $^\circ\text{C}$  indicated the portlandite decomposition, whilst the other which appeared at approximately 700  $^\circ\text{C}$  is due to the decarboxylation of calcite. Apparently, the peaks at 90-120  $^\circ\text{C}$  decreased as the slag content increased. This may be a part of the reason why as slag content increased the compressive

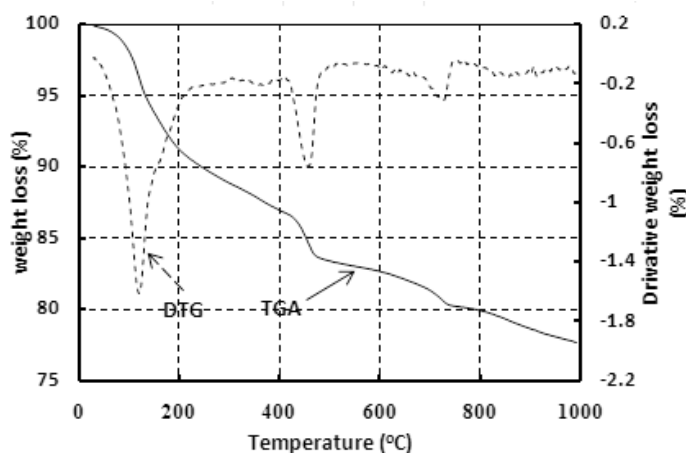


Fig. 8. TGA and DTG curve for neat PC after 28 days of hydration

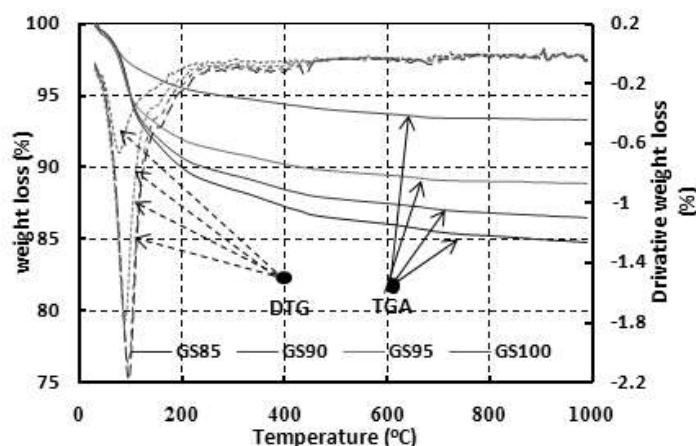


Fig. 9. TGA and DTG curve for HVS pastes after 28 days of hydration

strength decreased, at age of 28 days. The results of TGA/DTG are in agreement with that obtained by XRD.

### 3. 7. Microstructural Analysis

Figs. 10 and 11 show SEM micrographs of fracture surface of the hardened neat PC and HVS samples after 28 days of hydration. As shown in Fig. 10, the hydration products appear relatively dense and homogenous matrix. Some anhydrous particles are surrounded by rims of inner hydration products. The microstructures of the samples prepared from HVS are shown in Fig. 11. The angular of slag stand out in stark. It can be seen from the micrographs of GS85 (Fig. 11a) some very dark slag-like shaped voids. In GS85 sample, many anhydrous or partially hydrated slag grains remained. The hydrated cement gel was building up a matrix between the slag particles, hence reducing the porosity, in comparison with the other HVS samples that shown in Fig. 11b, c, d. It can be seen from Fig. 11a that a thin rim was formed around some of the slag particles, whilst the cement fraction had hydrated. The micrographs of fracture surface of the hardened GS90 and GS95 samples are presented in Fig. 11b, c. It can be seen that both of un-hydrated slag particles and voids increase as the slag content increases (i.e. un-hydrated

slag particles and voids are larger in GS95 followed by GS90 followed by GS90). In addition, the more slag grains of larger size were observed in GS90 and GS95 samples in comparison with that of GS85 sample. This may be a part of the reason why the 28 days compressive strength of the GS85 > GS90 > GS 95. The microstructure of GS100 (Fig. 11d) contains larger number of either anhydrous or partially hydrated slag particles and more slag grains of larger size, whilst the grains in the GS85 (Fig. 11a) seem to have more extensively broken

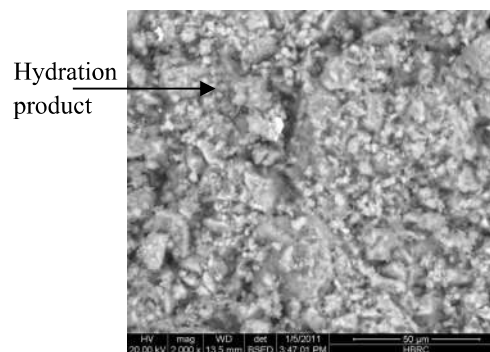


Fig. 10. SEM micrograph of fracture surface of hardened neat PC paste at age of 28 days

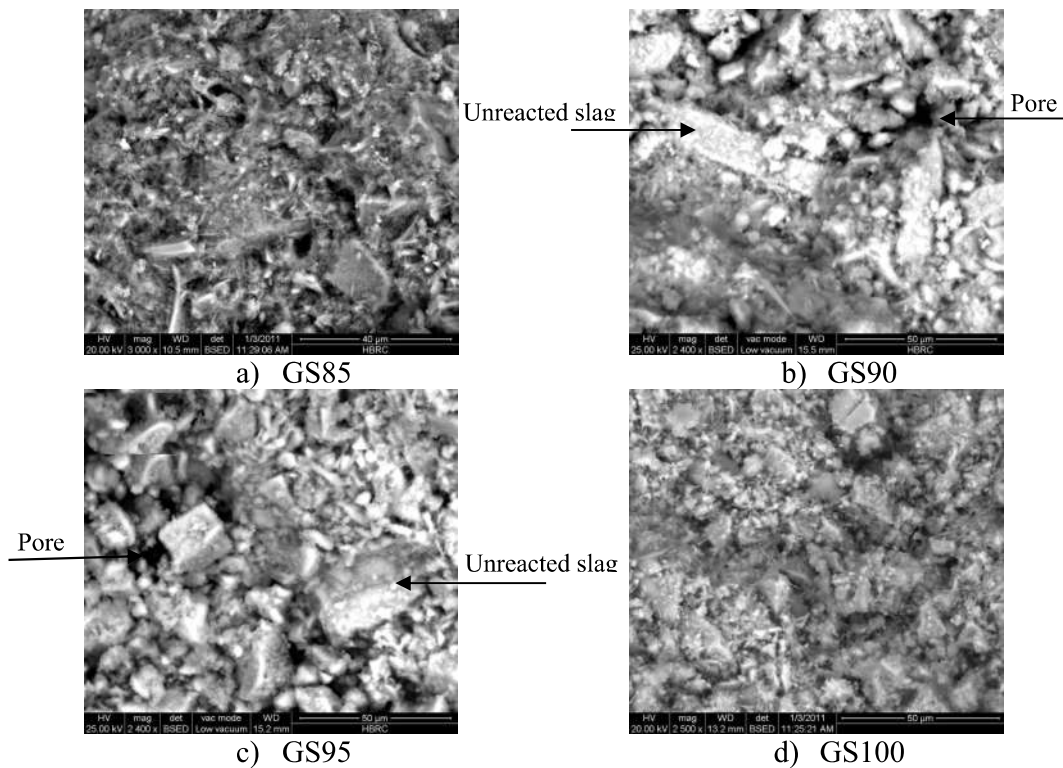


Fig. 11. SEM micrograph of fracture surface of hardened HVS pastes at age of 28 days

down. The micrograph of GS100 shows porous microstructure and the slag grains did not show rims, in comparison with that of GS85. This may be a part of the reason why the 28 days compressive strength of the GS85 > GS100.

### 3. 8. Drying Shrinkage

As known, shrinkage is the reduction in volume at constant temperature without external loading. It is as important material property that significant effects on long-term performance of designed structures. It also influences structural properties and durability of the material [1, 4, 5], of which drying shrinkage can be a major reason for deterioration of concrete structures. The contraction of the material is normally hindered by either internal or external restraints so that tensile stresses are induced. These stresses may exceed the tensile strength and cause concrete to crack. However, Fig. 12 presents shrinkage

observed for the neat PC and HVS pastes at slag levels of 85% and 90%. All the HVS paste specimens showed lower drying shrinkage from early age up to 60 days, whilst they showed larger drying shrinkage beyond 60 days compared to the

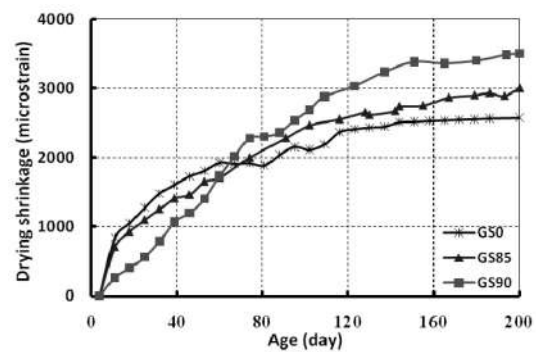


Fig. 12. Drying shrinkage of GS0, GS85 and GS90 paste prisms

neat PC paste specimen. Among the HVS pastes, the 90% replacement level showed the largest drying shrinkage and 85% showed the least. Ling and Poon [29] related the reduction in the drying shrinkage with the introduction of HVS to the consumption of free water and the decreasing in the amount of the evaporable water. In the literature, some authors [30] showed that 65% slag concrete mixture gave higher drying shrinkage than neat PC concrete. Fulton [31] indicated that the drying shrinkage of slag cement concrete at age of 3.5 years might be 40% higher than an equivalent PC mixture. Heaton [32] conducted tests on concretes containing 40% slag subjected to drying environment after 7 days of moist curing. The results showed that after 400 days of drying the shrinkage of concrete containing slag was 25% higher than that of PC concrete. On the contrary, other authors believed that slag concrete/mortar gave lower drying shrinkage than that of neat PC concrete/mortar, where Itim et al. [33] showed that the neat PC mortar gave larger drying shrinkage than 10%, 30% and 50% slag mortars. Their results indicated that as slag content increased as the drying shrinkage decreased. Güneyisi et al. [34] showed that 20%, 40% and 60% slag concrete exhibited lower drying shrinkage than neat PC concrete. The drying shrinkage decreased with increasing slag content. Jianyong and Yan [35] showed that 30% slag concrete exhibited lower drying shrinkage than the neat PC concrete. The work of Neville and Brooks [36] showed that for concretes subjected to a drying environment of 60% RH at 20 °C after a period of 28 days storage in water, the drying shrinkage of the 50% slag mixture was about 10% lower than the PC mixture. Bamforth [37] reported that in short term (i.e. approximately 50 days) concretes containing 70% slag had a lower rate of drying shrinkage than PC mixture, but that in the long term (i.e. up to 14 months) the rate of shrinkage was accelerated by the use of slag.

These differ in drying shrinkage results may be related to the difference in the magnitude and the evolution of the drying shrinkage from country to country and the data cannot be directly compared [38] In addition, a direct comparison of the results from different investigators is sometimes

difficult because of the differing condition under which the tests were carried out. However, clearly, more data required to establish the effect of curing period, fineness and slag composition on the shrinkage characteristics of the cement.

#### 4. CONCLUSIONS

This paper presents the first results on HVS paste mixtures where cement was replaced with slag up to 100%. The following conclusions are drawn from the test results and analysis presented in this investigation:

1. Paste workability was affected by slag content, where it increased with increasing slag content. The GS0 gave the lowest workability, whilst GS100 gave the highest workability.
2. The value pH was affected by slag content. The incorporation of 85% slag reduced the pH value of the neat PC sample by about 3%, whilst the incorporation of 100% reduced it by about 4.6%.
3. Generally, there was a systematic decrease in compressive strength with the increase in slag content, especially at early ages (i.e. the compressive strength of GS0 > GS85 > GS90 > GS95 > GS100); at latter age, GS100 gave higher strength than GS95.
4. Paste density decreased with increasing the slag content. The GS100 showed 9.14% reduction in the density in comparison with those of GS0.
5. HVS pastes (GS85 and GS90) showed lower drying shrinkage compared to GS0 up to age of 60 days, whilst they showed higher drying shrinkage beyond this age. The drying shrinkage increased as slag content increased (i.e. drying shrinkage of GS90 > GS85 > GS0).

#### REFERENCES

1. Rashad, A. M., "Properties of alkali-activated fly ash concrete blended with slag". *Iranian Journal of Materials Science & Engineering*, March 2013, 10, 1, 57-64.
2. Rashad, A. M. and Khalil, M. H., "A preliminary study of alkali-activated slag

- blended with silica fume under the effect of thermal loads and thermal shock cycles". *Construction and Building Materials*, 2013, 40, 522-532.
3. Rashad, A. M. and Zeedan, S. R., "The effect of activator concentration on the residual strength of alkali-activated fly ash pastes subjected to thermal load". *Construction and Building Materials*, 2011, 25, 3098-3107.
4. Rashad, A. M., "A comprehensive overview about the influence of different additives on the properties of alkali-activated slag – A guide for Civil Engineer". *Construction and Building Materials*, 2013, 47, 29-55.
5. Rashad, A. M., "A comprehensive overview about the influence of different admixtures and additives on the properties of alkali-activated fly ash. *Materials and Design*," 2014, 53, 1005-1025.
6. Rashad, A. M., "Alkali-activated metakaolin: A short guide for Civil Engineer – An overview". *Construction and Building Materials*, 2013, 41, 751-765.
7. Rashad, A. M., Metakaolin as cementitious material: History, sources, production and composition – A comprehensive overview. *Construction and Building Materials*, 2013, 41, 303-318.
8. Chen, C., Habert, G., Bouzidi, Y. and Julien, A., "Environmental impact of cement production: detail of the different processes and cement plant variability evaluation". *Journal of Cleaner Production*, 2010, 18, 5, 478-485.
9. Rashad, A. M., Bai, Y., Basheer, P. A. M., Collier, N. C. and Milestone, N. B., "Chemical and mechanical stability of sodium sulfate activated slag after exposed to elevated temperature". *Cement and Concrete Research*, 2012, 42, 333-343.
10. Rashad, A. M., Bai, Y., Basheer, P. A. M., Milestone, N. B., and Collier, N. C., "Hydration and properties of sodium sulfate activated slag". *Cement & Concrete Composites*, 2013, 37, 20-29.
11. Gartner, E., "Industrially interesting approaches to "low-CO<sub>2</sub>" cements". *Cement and Concrete Research*, 2004, 34, 1489-1498.
12. Mehta, P. K., "Global concrete industry sustainability: tools for moving forward to cut carbon emissions" In: *Concrete international*, February 2009, 45-8.
13. Rashad, A. M., Seleem, H. E. D. and Yousry, K. M., "Compressive strength of concrete mixtures with binary and ternary cement blends". *Building Research Journal*, 2009, 57, 2, 107-130
14. Seleem, H. E. D., Rashad, A. M. and Elsokary, T., "Effect of elevated temperature on physic-mechanical properties of blended cement concrete". *Construction and Building*, 2011, 25, 1009-1017.
15. Kuder, K., Lehman, D., Berman, J., Hannesson, G. and Shogren, R., "Mechanical properties of self consolidating concrete blended with high volumes of fly ash and slag". *Construction and Building Materials*, 2012, 34, 285-295.
16. Rashad, A. M., "An investigation on very high volume slag pastes subjected to elevated temperatures". *Construction and Building Materials*, 2015, 74, 249-258.
17. Rashad, A. M. and Sadek, D. M., "An investigation on Portland cement replaced by high-volume GGBS pastes modified with micro-sized metakaolin subjected to elevated temperatures". *International Journal of Sustainable Built Environment*, 2017, 6, 91-101.
18. Rashad, A. M., El-Nouhy, H. A. and Zeedan, S. R., "An investigation on HVS paste modified with nano-SiO<sub>2</sub> impervious to elevated temperatures". *Arabian Journal for Science and Engineering*, Published on line 29 November 2017, <https://doi.org/10.1007/s13369-017-2985-1>.
19. British Standards Institution, Method determination of density of hardened concrete, BSI, London, 1983, BS 1881: Part 114.
20. Wei, S., Handong, Y. and Binggen, Z., "Analysis of mechanism on water-reducing effect of fine ground slag, high-calcium fly ash, and low-calcium fly ash". *Cement and Concrete Research*, 2003, 33, 1119-1125.
21. Linnu, L. U., Yongjia, H. E., Shuguang, H. U., "Binding materials of dehydrated phases of waste hardened cement paste and pozzolanic admixture". *Journal of Wuhan University of Technology-Mater. Sci. Ed.*, Feb. 2009, 24, 1, 140-144.
22. Atiş, C. D. and Bilim, C., "Wet and dry compressive strength of concrete containing

- ground granulated blast-furnace slag". *Building and Environment*, 2007, 42, 3060-3065.
23. Güneyisi, E. and Gesoğlu, M., "A study on durability properties of high-performance concretes incorporating high replacement levels of slag". *Materials and Structures*, 2008, 41, 479-493.
24. Miura, T. and Iwaki, I., "Strength development of concrete incorporating high levels of ground granulated blast-furnace slag at low temperature". *ACI Materials Journal*, January-February 2000, 97-M09, 66-71.
25. Joo, H. H. and Yong, H. C., "Physico-chemical properties of protein-bound polysaccharide from *Agaricus blazei* Murill prepared by ultrafiltration and spray drying process". *Int. J. Food Sci. Technol.* 2007, 42, 1-8.
26. Rashad, A. M., Zeedan, S. R. and Hassan, A. H., "A preliminary study of autoclaved alkali-activated slag blended with quartz powder". *Construction and Building materials*, 2012, 33, 70-77.
27. Mojudar, S. C. and Janokta, I., "Thermophysical properties of blends from Portland and sulphoaluminate-belite cements". *Acta Phys Slovaca*, 2002, 52, 5, 435-46.
28. Rashad, A. M. and Zeedan, S. R., "A preliminary study of blended pastes of cement and quartz powder under the effect of elevated temperature". *Construction and Building Materials*, 2012, 29, 672-681.
29. Ling, T. C. and Poon, C. S., "Feasible use of large volumes of GGBS in 100% recycled glass architectural mortar". *Cement & Concrete Composites*, 2014, 53, 350-356.
30. Aly, T. K. and Sanjayan, J. G., "Effect of gypsum on free and restrained shrinkage behavior of slag-concretes subjected to various curing conditions". *Materials and Structures*, 2008, 41, 1393-1403.
31. Fulton, F. S., "The properties of Portland cements containing milled granulated blastfurnace slag". *South African Portland Cement Institute Monograph*, Johannesburg, 1974.
32. Heaton, B. D., "Characteristics of concrete with partial cement replacement by fly ash and ground granulated blast furnace slag Symp". *On Concrete Cases and Concepts*, Canberra, Inst. Of Engrs. Of Australia, 1979, 26-30.
33. Itim, A., Ezziane, K. and El-Hadj, K., "Compressive strength and shrinkage of mortar containing various amounts of mineral additions. *Construction and Building Materials*", 2011, 25, 3603-3609.
34. Güneyisi, E., Gesoğlu, M. and Özbay, E., "Strength and drying shrinkage properties of self-compacting concretes incorporating multi-system blended mineral admixtures". *Construction and Building Materials*, 2010, 24, 1878-1887.
35. Jianyong, L. and Yan, Y., "A study on creep and drying shrinkage of high performance concrete". *Cement and Concrete Research*, 2001, 31, 1203-1206.
36. Neville, A. M. and Brooks, J. J., *Time-dependent behaviour of Cemsave concrete*. Concrete, 1975, 9, 3, 36-39.
37. Bamforth, P. B., "An investigation into the influence of partial Portland cement replacement using either fly ash or granulated blast furnace slag on the early age and long term behaviour of concrete". *Internal Report No. 014J/78/2067*, Taylor Woodrow Southhall, England, 1978.
38. Videla, C. and Aguilar, C., "An update look at drying shrinkage of Portland and blended Portland cement concretes". *Magazine of Concrete Research*, 7, 2006, 58, 459-476.